Dynamic Order-Disorder in Atomistic Models of Structural Glass Formers

Lester O. Hedges,[1]* Robert L. Jack,[1,2]* Juan P. Garrahan,[3] David Chandler[1]†

The glass transition is the freezing of a liquid into a solid state without evident structural order. Although glassy materials are well characterized experimentally, the existence of a phase transition into the glass state remains controversial. Here, we present numerical evidence for the existence of a novel first-order dynamical phase transition in atomistic models of structural glass formers. In contrast to equilibrium phase transitions, which occur in configuration space, this transition occurs in trajectory space, and it is controlled by variables that drive the system out of equilibrium. Coexistence is established between an ergodic phase with finite relaxation time and a nonergodic phase of immobile molecular configurations. Thus, we connect the glass transition to a true phase transition, offering the possibility of a unified picture of glassy phenomena.

When supercooled far below their melting temperatures, many liquids become extremely viscous, so much so that at low enough temperatures these materials become amorphous solids (*1*, *2*). This phenomenon is termed the "glass transition." The dynamical behavior of molecules in a glass is heterogeneous in that there are domains of mobile and immobile molecules segregated in space (*3*–*6*). At equilibrium, the spatial extent of these domains is large compared with molecular dimensions (*5*) but not so large to imply an actual phase transition. Indeed, and despite the name given to it, there is no observation that demonstrates a link between the glass transition and a phase transition controlled by traditional thermodynamic variables like temperature and pressure.

Nevertheless, for idealized lattice models, recent work has established the existence of a nontraditional phase transition, one controlled by variables that drive a system out of equilibrium (*7*–*9*). Here, we present numerical evidence for the same behavior in atomistic models of structural glass formers. We do so with a suitable form of transition path sampling (*10*) that allows us to study ensembles of long trajectories for supercooled fluids with several hundred particles driven out of equilibrium by a field that couples to their mobility. By adjusting field strength, trajectories of these supercooled fluids can be moved reversibly between ergodic and nonergodic behaviors. The former are mobile states with finite relaxation times: the system forgets its initial state. The latter are immobile states that remember initial conditions for all time. At intermediate field strengths, trajectory space is filled by two coexisting domains, one that is ergodic and one that is nonergodic.

In this way, it appears that dynamic heterogeneity observed in the equilibrium dynamics of supercooled fluids is a precursor to a first-order phase transition in space-time. First-order transitions are associated with a discontinuity in an order parameter and a corresponding singularity in a partition function, such as the discontinuity in density for a liquid-vapor transition. These mathematical features emerge from the principles of statistical mechanics in the limit of a very large system, what is usually called the "thermodynamic" limit (*11*). For finite systems studied numerically, there are no such singularities. Evidence of a phase transition in these cases is found in the behaviors of crossovers from one phase to another (*12*). Figure 1 illustrates the system-size behavior of a crossover. For the transition we consider, the partition function is a sum over dynamical histories (i.e., trajectories) of the system, and the order parameter measures the amount of activity or mobility that occurs among N particles in a volume V with trajectories that run for an observation time, t_{obs}. As such, the pertinent measure of system size is a volume in space-time, the product $N \times t_{obs}$ or equivalently $V \times t_{obs}$. In the work reported here, we consider spatial volumes that are 10 to 30 times larger than the correlation volume of the equilibrium system and observation times that are 10 to 100 times longer than a structural relaxation time of the undriven system. These sizes are sufficient to exhibit behaviors suggestive of a nonequilibrium phase transition.

Equilibrium and nonequilibrium phase transitions. To discuss how these behaviors are revealed, let us first recall how Gibbs' statistical mechanics is used to study traditional equilibrium phase transitions (*11*). Taking a system of N particles at a pressure p, we use the volume V as an order parameter and take microstates to be points in configuration space, $x = (\mathbf{r}_1, \mathbf{r}_2, ..., \mathbf{r}_N)$, where the vector $\mathbf{r}_i$ denotes the position of the ith particle. Different phases, such as liquid and vapor, are distinguished from the other by the typical size of V. Changes in V are coupled to the thermodynamic field p or βp, where $1/\beta$ stands for Boltzmann's constant times temperature, $k_B T$. In particular, the probability of a configuration, x, is proportional to $P_0(x)\exp[-\beta \Delta p V(x)]$, where $P_0(x)$ is the probability of x at the reference field or pressure $p_0 = p - \Delta p$. The mean volume of the system with this distribution is $\langle V \rangle_p \equiv V_p$, which is depicted schematically in Fig. 1. A first-order phase transition is manifested by a discontinuity at the pressure $p = p^*$. At this value of the pressure, two phases coexist with respective volumes per particle v_1 and v_2.

At coexistence, the distribution function for the order parameter is bimodal. The two peaks in the distribution coincide with the two equilibrium phases. There is a low probability to observe an intermediate value of V, between Nv_1 and Nv_2 in Fig. 1. This low probability decreases exponen-

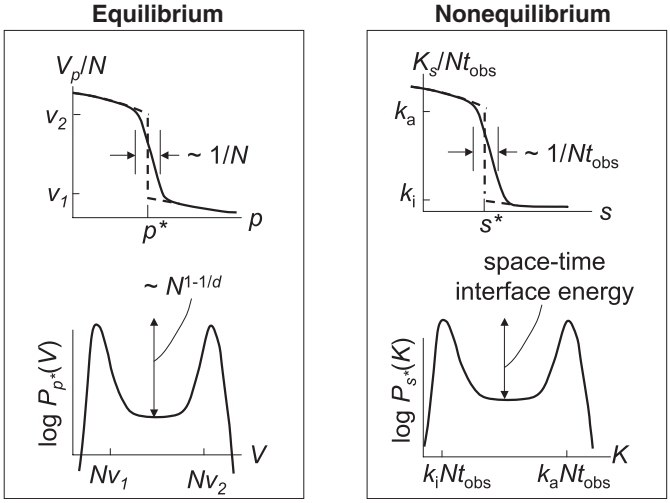

Fig. 1. Finite size effects of equilibrium and nonequilibrium phase transitions. The mean volume V_p manifests an equilibrium first-order phase transition at pressure $p = p^*$, whereas the mean dynamical activity K_s manifests a dynamical first-order phase transition at the dynamical field $s = s^*$. At conditions of phase coexistence, the volume distribution function, $P_p(V)$, and the dynamical activity distribution, $P_s(K)$, are bimodal. Configurations or trajectories with intermediate behaviors lie at much higher free energies (lower probabilities) than those of the basins. For finite systems, discontinuous phase transitions become crossovers with widths that vanish as system size, N, and observation time, t_{obs}, grow to infinity.

[1]Department of Chemistry, University of California, Berkeley, CA 94720–1460, USA. [2]Department of Physics, University of Bath, Bath BA2 7AY, UK. [3]School of Physics and Astronomy, University of Nottingham, Nottingham NG7 2RD, UK.

*These authors contributed equally to this work.
†To whom correspondence should be addressed. E-mail: chandler@cchem.berkeley.edu

tially with the free energy cost to form an interface between the phases. The interfacial free energy grows as $N^{1-1/d}$, where d is the dimensionality. In the limit of a large system, therefore, volumes between Nv_1 and Nv_2 can be achieved only through a direct constraint on the volume. Further, at coexistence, the presence of two macroscopic states means that the mean square fluctuation in the volume grows as N^2. Because the response of the volume to a change in pressure is $-\partial V_p/\partial p = k_B T\langle(V - V_p)^2\rangle_p$, these large fluctuations mean that the width of the crossover illustrated in Fig. 1 vanishes as $1/N$.

Analogous statements for trajectory space begin with a choice of order parameter, which we have taken to be

$$K[x(t)] = \Delta t \sum_{t=0}^{t_{obs}} \sum_{j=1}^{N} |\mathbf{r}_j(t + \Delta t) - \mathbf{r}_j(t)|^2$$

where $\mathbf{r}_j(t)$ and $x(t)$ refer to particle position and point in configuration space, respectively, now as functions of time t. This chosen order parameter depends on the system's path or history over the observation period, $0 \le t \le t_{obs}$. Square brackets are used to indicate that the order parameter is a function of configurations $x(t)$ over the entire period. The incremental time, Δt, is assigned a value for which a particle in a normal liquid would typically move a distance of the order of a molecular diameter. The sum over time is done incrementally, every Δt, thus giving a total of $t_{obs}/\Delta t$ points in time that contribute. When particles are mobile, as in a normal liquid, $K[x(t)]$ is typically large; when particles are immobile, as in a glass, $K[x(t)]$ is typically small. An order-disorder transition reflecting extensive changes in particle mobility is reflected in a discontinuous mean value of $K[x(t)]$.

The next step is to consider the probability distribution for trajectories when this order parameter is coupled to a field s (*13*, *14*). This distribution is proportional to $P_0[x(t)]\exp\{-sK[x(t)]\}$, where $P_0[x(t)]$ is the equilibrium probability distribution, that is, the distribution at $s = 0$. The equilibrium distribution is for trajectories that are causal and time-reversal symmetric and that preserve an equilibrium distribution of microstates. Its partition function is trivial because the distribution is normalized, that is, $1 = \sum_{x(t)} P_0[x(t)]$, where the sum over $x(t)$ is a sum over all trajectories. In contrast, the perturbed distribution

$$P_s[x(t)] \propto P_0[x(t)]\exp\{-sK[x(t)]\}$$

has a nontrivial partition function, which for positive s decreases with increasing t_{obs}. For the space of trajectories governed by that distribution at positive s, this space is compressed with increasing t_{obs}, and, for large enough s, configurations favored by that distribution are ones that are visited by immobile or nonergodic trajectories. $P_s[x(t)]$ is therefore a distribution for trajectories of a system driven out of equilibrium.

Laboratory procedures for forming glass are nonequilibrium processes that stabilize configurations from which equilibration is impossible. One example is the preparation of ultrastable glasses via vapor deposition (*15*). We use the field s as a mathematical device to access these same configurations, configurations that would have negligible statistical weight in an undriven equilibrium dynamics. We do not address how a particular experimental protocol stabilizes these nonergodic configurations. We do, however, address whether the domain of these configurations is sufficiently large to produce a nonequilibrium phase transition.

Transition path sampling of the *s* ensemble. In ordinary molecular dynamics or Monte Carlo trajectories of model systems, trajectories obey detailed balance and are presumed to be ergodic. Their distribution, $P_0[x(t)]$, can be sampled by either running a single trajectory for a time $n \times t_{obs}$ or equivalently carrying out a random walk through trajectory space, sampling n independent trajectories each of duration t_{obs}. The latter procedure is a method of transition path sampling (*10*). To sample $P_s[x(t)]$, we use transition path sampling but now accepting or rejecting random walk steps so as to preserve the weight $P_0[x(t)]\exp\{-sK[x(t)]\}$. We call the collection of trajectories harvested in this way the "s ensemble." In this ensemble, for models with sufficiently correlated dynamics, the distribution function for the order parameter can be bimodal, as indicative of an order-disorder transition (*7*–*9*). This behavior is illustrated schematically in Fig. 1 in a fashion that stresses its analogy with the corresponding behavior of an equilibrium phase transition.

In particular, the average value of the order parameter we have chosen is extensive in space-time, that is, $K_s = \langle K[x(t)]\rangle_s$ is proportional to $N \times t_{obs}$, where the proportionality constant is the

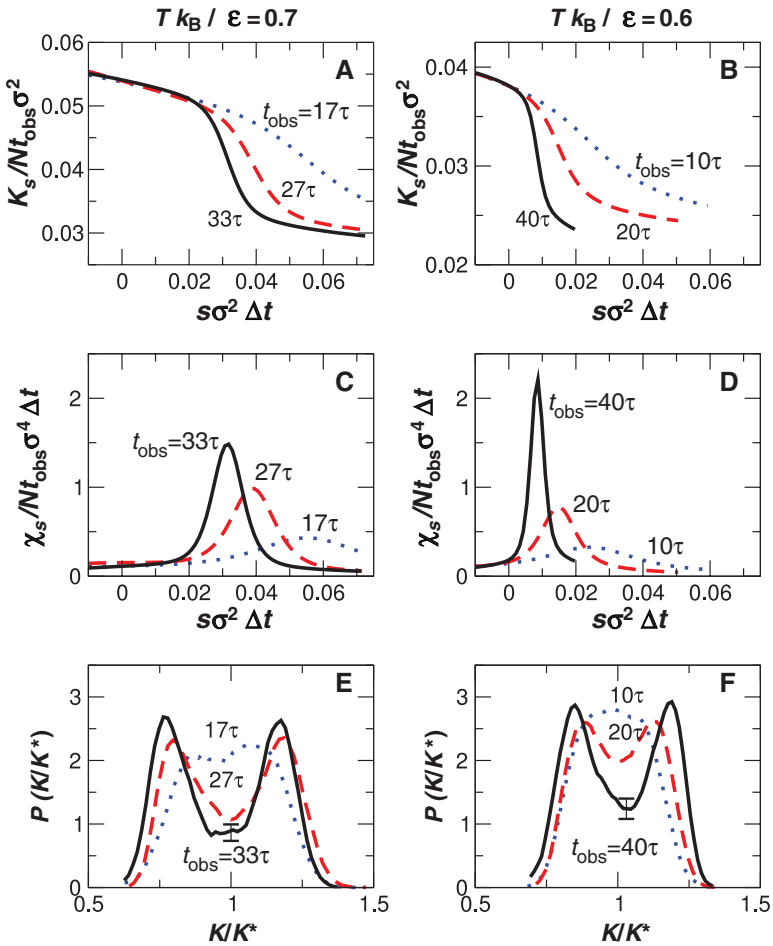

Fig. 2. Evidence for first-order phase transition in space-time. (**A** and **B**) Average space-time order parameter $K_s = \langle K[x(t)]\rangle_s$ as a function of field s, from molecular dynamics simulations of the KA Lennard-Jones mixture for $N = 150$ total particles, at reduced temperatures $k_BT/\varepsilon = 0.6$ and $k_BT/\varepsilon = 0.7$, and principal component density $N_A\sigma^3/V = 0.96$. ε and σ are the Lennard-Jones parameters for the larger (principal component) particles in the KA mixture. As the length of trajectories increases, the crossover in K_s becomes sharper and happens at smaller values of s. (**C** and **D**) The peak in the susceptibility $\chi_s = \frac{\partial K_s}{\partial s}$ becomes larger, and its position moves to smaller s with increasing t_{obs}. The crossover of K_s reflects a first-order transition in the infinite size limit. (**E** and **F**) Distribution of K at coexistence (where $K^* = K_s$ for $s = s^*$). For large t_{obs}, the order parameter distribution at the coexistence field s^* becomes bimodal, as expected for a first-order transition.

mean-square displacement of a particle in an incremental time Δt. If two dynamical phases coexist, one with proportionality constant k_a and the other with k_i, then K_s will be a discontinuous function of s at the condition of coexistence, $s = s^*$. As illustrated with Fig. 1 for a finite system, the corresponding crossover will have width of the order of $1/Nt_{obs}$ because the mean square fluctuations in the order parameter grow as $(Nt_{obs})^2$. Further, the excess in free energy to maintain a coexisting ensemble grows as an interfacial area in space-time, so that trajectories manifesting this coexistence are suppressed by a factor that depends exponentially on this area. In some cases (*8*), this area scales as $N^{1-1/d}t_{obs}$. The value s^* is proportional to the rate at which configurations from the nonergodic "inactive" phase relax back to the ergodic equilibrium fluid if the driving field s is removed. In kinetically constrained lattice models (*9*), which are idealized models of structural glass formers (*16*), this rate is zero, that is, $s^* = 0$. In other words, for those models, undriven equilibrium dynamics coexists with a nonergodic phase. Here, we show that for more realistic atomistic models, and therefore for real glass forming materials, s^* is small although perhaps nonzero.

The particular system we have considered is Kob and Andersen's (KA) two-component mixture of Lennard-Jones particles (*17*). It has $N_A = 0.8N$ principal particles, each with Lennard-Jones diameter σ and energy parameter ε. In addition, it has $N_B = 0.2N$ smaller secondary particles, where their size and attractive energy parameters are chosen so as to frustrate crystallization (*17*). The structural and dynamical properties we report for this model, including the order parameter $K[x(t)]$, refer to the principal particles. We have carried out two independent studies, one where trajectories are governed by Newtonian molecular dynamics and the other where trajectories are governed by a Monte Carlo dynamics. With appropriate scaling of time, both studies yield similar results. The results shown in the figures of this paper are from the molecular dynamics studies. For the incremental time, we use $\Delta t = 13.33(m\sigma^2/48\varepsilon)^{1/2}$, where m is the mass of the particles. Results from the Monte Carlo dynamics plus additional information about our computations are presented in (*18*). In terms of the reduced temperature k_BT/ε, the KA model behaves as an ordinary simple fluid at temperatures $k_BT/\varepsilon > 1$, but its relaxation slows and large glassy fluctuations appear at lower temperatures. Around $k_BT/\varepsilon = 0.4$, relaxation becomes so slow that equilibration of the model on current-day computers becomes intractable. For what is shown below, we work at less severe but nonetheless nontrivial supercooled conditions, $0.6 \leq k_BT/\varepsilon \leq 0.7$.

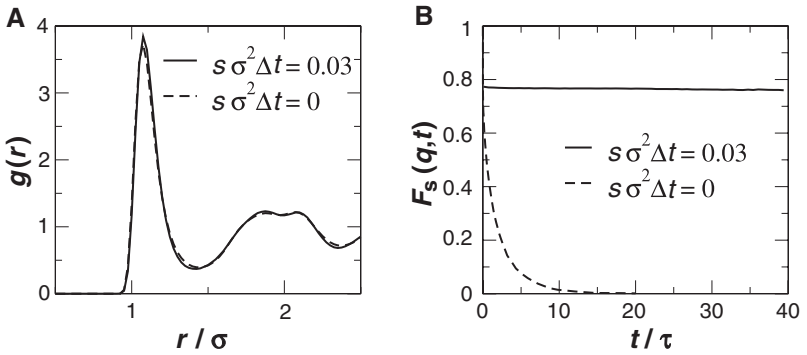

Fig. 3. Comparison of structure and dynamics of active and inactive phases. (**A**) Radial distribution function for the atoms of the principal component in the KA mixture. The equilibrium KA mixture is at $s = 0$. The nonequilibrium mixture is at $s = 0.03/\sigma^2\Delta t > s^*$. Here, σ is the Lennard-Jones diameter for the principal component atoms, and $\Delta t = 13.33(m\sigma^2/48\varepsilon)^{1/2} \simeq \tau/15$, where τ is the structural relaxation time. There is no appreciable difference in the static structures of the active, $s < s^*$, and inactive, $s > s^*$, dynamical phases. (**B**) Self-intermediate scattering function for the same values of s. In the active phase, correlation functions relax to zero. In the inactive phase, correlation functions remain at a nonzero value even for the longest times; the inactive phase is nonergodic. These results were obtained by using simulations of $N = 150$ total particles, at reduced temperature and principal component density $k_BT/\varepsilon = 0.6$ and $N_A\sigma^3/V = 0.96$, respectively.

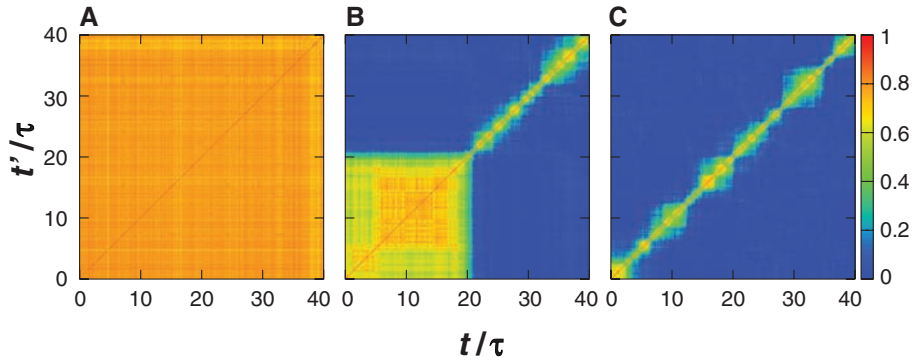

Fig. 4. Space-time interface at phase coexistence. Representative overlap matrices $Q(t,t') = N^{-1}\sum_{i=1}^{N}\cos\{\mathbf{q} \cdot [\mathbf{r}_i(t) - \mathbf{r}_i(t')]\}$ taken from the ensemble of trajectories at the coexistence field s^*, for $k_BT/\varepsilon = 0.6$, $t_{obs} = 40\tau$ and $N = 150$ (Fig. 2B). (**A**) Typical trajectory from the inactive phase (from the low K_s peak in Fig. 2F), where for all observation times the correlation function remains close to 1, indicating nonergodic dynamics. (**B**) Typical trajectory at coexistence (for values of K_s in the trough of Fig. 2F), where the overlap matrix shows a sharp interface-like structure at $t/\tau \approx 20$ separating an inactive region of space-time at earlier times and an active region at later times. (**C**) Typical trajectory from the active phase (from the high K_s peak in Fig. 2F), where the system's dynamics is ergodic and the correlation function decays rapidly to zero. The inhomogeneous features evident in (C) are finite size effects that would vanish in the limit of infinite size, $N \to \infty$.

Bistability and phase transition in trajectory space. Our findings for the mean order parameter and its distribution in the s ensemble (Fig. 2) reflect the qualitative features associated with a first-order phase transition. The quantitative analysis of finite-size scaling is beyond the capabilities of the algorithms we have used in this work, but the results we have obtained are similar to those established in idealized kinetically constrained models of glass formers (*7*–*9*). The susceptibility

$$\chi_s = -\frac{\partial K_s}{\partial s} = \langle\{K[x(t)] - K_s\}^2\rangle_s$$

has a peak that grows with increasing N and t_{obs}. The peak position is the finite system estimate of s^* (*20*). Its value decreases with increasing N and t_{obs} [system size scaling shown in (*18*)]. The order parameter distribution is bimodal at this value of s, and the minimum between its two peaks decreases with increasing N and t_{obs}. For

the range of values of N and t_{obs}, the effects of increasing t_{obs} are greater than those of increasing N. This asymmetry in the dependence on N and t_{obs} is also reflected in the structure of space-time at coexistence. We will describe this structure but first discuss a measure of ergodicity.

The particular measure we consider is the behavior of the function

$$F_s(q,t) = \frac{1}{Nt_{obs}} \sum_{t'=0}^{t_{obs}} \sum_{i=1}^{N} \langle \exp\{i\mathbf{q}\bullet[\mathbf{r}_i(t+t') - \mathbf{r}_i(t')]\}\rangle_s$$

At equilibrium, that is, $s = 0$, $F_s(q, t)$ is the Van Hove self-correlation or intermediate-scattering function (*21*). In general, it is a mean overlap between configurations displaced by a time t. The extent to which it is nonzero in the limit of large t is a measure of nonergodicity (*22*). We choose the wave vector q to coincide with the first maximum in the structure factor of the liquid (or glass). With this choice, the time τ for which $F_0(q, \tau) = 1/e$ is a common definition of the structural relaxation time. $F_s(q, t)$ is shown in Fig. 3 for the active (i.e., ergodic) and inactive (i.e., nonergodic) phases. The relaxation time of the active trajectories is much less than t_{obs}, yet inactive trajectories remain trapped in a single state throughout the observation time. Figure 3 also shows the radial distribution function for the principal component of the mixture in the active and inactive states. This average measure of structure in the phase that can equilibrate ($s = 0$) is virtually identical to that for the phase that is driven to a nonergodic state ($s > 0$). Thus, fluctuations from the mean structure are crucial to the difference between glassy and fluid materials.

Figure 4 illustrates the structure of trajectory space at conditions of active-inactive coexistence, that is, at $s = s^*$. Each panel illustrates an overlap matrix,

$$Q(t,t') = N^{-1} \sum_{i=1}^{N} \cos\{\mathbf{q}\bullet[\mathbf{r}_i(t) - \mathbf{r}_i(t')]\},$$

and records the similarity or overlap on a given trajectory between configurations at different times t and t'. The s ensemble average of this quantity gives $F_s(q, t - t')$. The pictures in Fig. 4 illustrate the fluctuations from the mean, with the distance from the diagonal reflecting the time interval $t - t'$. At $s = s^*$, there are some trajectories with relatively high values of K indicative of the active phase, others with relatively low values indicative of the inactive phase, and lastly those that are intermediate and that demonstrate phase coexistence. Figure 4C shows a representative trajectory with a value of K corresponding to the active phase; see Fig. 2F. Here, motion is plentiful, and the system quickly decorrelates as $t - t'$ grows.

In contrast, the overlap matrix for inactive trajectories, as illustrated in Fig. 4A, is homogeneous. The system remains correlated for the entire observation time, so that $Q(t, t')$ is large even when $|t - t'|$ is much greater than a structural relaxation time τ. Figure 4B shows a trajectory where the active and inactive phases are separated by a sharp temporal interface. These figures might seem to resemble those found for trajectories of small equilibrium subsystems over time periods that are small compared with the structural relaxation time (*23*, *24*). However, overlap matrices for trajectories of an equilibrated system reveal a structure in space-time in which the system undergoes multiple transitions between collections of states with low energy and activity, commonly termed "meta-basins." Typical lifetimes for these inactive basins are of the order of a fraction of τ. These lifetimes are negligible compared with the very long lifetimes of inactive states within the s ensemble.

Figure 5 illustrates the correlations between the order parameter K and the behaviors of potential energy and icosahedral ordering at the coexistence field s^*. The potential energy of the inactive configurations is smaller, consistent with their stability. For active trajectories, particles sample many configurations, which leads to the self-averaging of structural measures and is reflected in the width of the distribution, which is significantly narrower for greater values of K. However, a clear correlation between potential energy and dynamics does not imply a causal link. Indeed, this thermodynamic variable cannot control the first-order transition that we describe here. Rather, we must look to variables that measure dynamics over a period of time. Although there is a gradual increase in icosahedral ordering (*19*) as K decreases, the observed correlation is far weaker than that of the potential energy. The broad distribution at small K is once again indicative of fluctuation dominance within the inactive phase.

Fluctuations, wetting, and critical points. The existence of a first-order transition has many consequences. For example, fluctuations in an equilibrium system near to phase coexistence grow rapidly as the surface tension between these phases is reduced. Figure 2 indicates that the KA mixture is near a coexistence line between active and inactive phases at both of the temperatures that we considered. Further, as the temperature is reduced, the values of K for the two phases approach each other, indicating that the surface tension between the phases will decrease as temperature decreases. We may therefore associate this decrease with the growth of fluctuations within the active phase. These fluctuations are the dynamical heterogeneities (*5*, *6*) in the equilibrium dynamics of the glass former. A further consequence of phase coexistence is the occurrence of wetting phenomena (*25*). In the case of the dynamical transition discussed here, "wetting" is remembering the initial conditions, and an example of this behavior can be seen for $F_s(q, t)$ in Fig. 3B. At $s > s^*$, the initial time surface is fully wetted by the inactive phase. At $s = 0 < s^*$, there is only a precursor to the wetting transition, a film of finite thickness in time.

For some idealized kinetically constrained models (*7*–*9*), coexistence between active and inactive phases along the $s = 0$ line ends at a $T = 0$ critical point. We expect similarly that, for the KA mixture, the order parameters of both the active and inactive phases will approach the same value, $K_s \to 0$ as $T \to 0$ and $s = 0$. However, where active-inactive coexistence is present in the kinetically constrained models for all temperatures when $s = 0$, the same cannot be true for models with finite intermolecular forces. At high enough temperatures, such forces are insufficiently

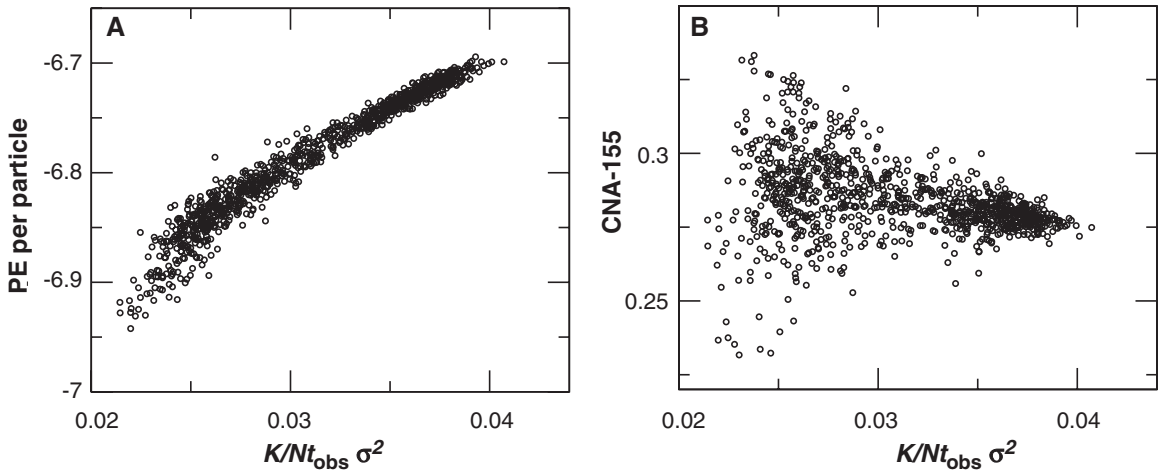

Fig. 5. Test of correlation between space-time order parameter and potential energy and icosahedral order. (**A**) Potential energy per particle in units of ε versus dynamical order parameter K of a trajectory. (**B**) Icosahedral order, as quantified by the CNA-155 parameter of the common neighbor analysis, as a function of K. Results are for trajectories at $k_BT/\varepsilon = 0.6$, $t_{obs} = 40\tau$, and $N = 150$.

constraining to produce collective behavior. Indeed, we have found that at small values of s, the order parameter distribution for the KA mixture ceases to be bimodal when k_BT/ε is significantly larger than 1 (*18*). One possibility is that the first-order coexistence line ends at an upper critical point at finite s and T. This possibility remains to be investigated.

The first-order transition we have described is to be contrasted with the scenario that emerges from other approaches, such as mode-coupling theory (*26*, *27*) and the random first-order transition theory (*28*, *29*). These theories predict the existence of dynamic or thermodynamic transitions controlled by thermodynamic fields such as temperature or pressure. In contrast, our results show that the order-disorder transition is in the trajectories of the dynamics and is thus controlled by dynamic fields. Perhaps a thermodynamic manifestation can be related to the picture of an avoided phase transition (*30*). In any case, our numerical results here suggest that in real glass formers this dynamical order-disorder phenomenon is close to that predicted from idealized kinetically constrained models (*7*–*9*). Thus, we pass the baton to the experimenters to find protocols for controlling the dynamic observable K or driving field s that allow experimental probes of the transition described in this work.

References and Notes

1. M. D. Ediger, C. A. Angell, S. Nagel, *J. Phys. Chem.* **100**, 13200 (1996).
2. P. G. Debenedetti, F. H. Stillinger, *Nature* **410**, 259 (2001).
3. K. Schmidt-Rohr, H. Spiess, *Phys. Rev. Lett.* **66**, 3020 (1991).
4. E. R. Weeks, J. C. Crocker, A. C. Levitt, A. Schofield, D. A. Weitz, *Science* **287**, 627 (2000).
5. M. D. Ediger, *Annu. Rev. Phys. Chem.* **51**, 99 (2000).
6. S. C. Glotzer, *J. Non-Cryst. Solids* **274**, 342 (2000).
7. M. Merolle, J. P. Garrahan, D. Chandler, *Proc. Natl. Acad. Sci. U.S.A.* **102**, 10837 (2005).
8. R. L. Jack, J. P. Garrahan, D. Chandler, *J. Chem. Phys.* **125**, 184509 (2006).
9. J. P. Garrahan *et al.*, *Phys. Rev. Lett.* **98**, 195702 (2007).
10. P. G. Bolhuis, D. Chandler, C. Dellago, P. L. Geissler, *Annu. Rev. Phys. Chem.* **53**, 291 (2002).
11. D. Chandler, *Introduction to Modern Statistical Mechanics* (Oxford Univ. Press, Oxford, 1987).
12. D. P. Landau, K. Binder, *A Guide to Monte Carlo Simulations in Statistical Physics* (Cambridge Univ. Press, Cambridge, 2000); see section 4.2.3.
13. J.-P. Eckmann, D. Ruelle, *Rev. Mod. Phys.* **57**, 617 (1985).
14. V. Lecomte, C. Appert-Rolland, F. van Wijland, *J. Stat. Phys.* **127**, 51 (2007).
15. S. F. Swallen *et al.*, *Science* **315**, 353 (2007); published online 6 December 2006 (10.1126/science.1135795).
16. F. Ritort, P. Sollich, *Adv. Phys.* **52**, 219 (2003).
17. W. Kob, H. C. Andersen, *Phys. Rev. Lett.* **73**, 1376 (1994).
18. Supporting materials are available for this article on *Science* Online.
19. J. D. Honeycutt, H. C. Andersen, *J. Phys. Chem.* **91**, 4950 (1987).
20. C. Borgs, R. Kotecky, *Phys. Rev. Lett.* **68**, 1738 (1992).
21. J. P. Hansen, I. R. McDonald, *The Theory of Simple Liquids* (Academic Press, London, 2006).
22. S. F. Edwards, P. W. Anderson, *J. Phys. F* **5**, 965 (1975).
23. B. Doliwa, A. Heuer, *Phys. Rev. E* **67**, 031506 (2003).
24. G. A. Appignanesi, J. A. Rodríguez Fris, R. A. Montani, W. Kob, *Phys. Rev. Lett.* **96**, 057801 (2006).
25. H. Nakanishi, M. E. Fisher, *Phys. Rev. Lett.* **49**, 1565 (1982).
26. W. Gotze, L. Sjogren, *Rep. Prog. Phys.* **55**, 241 (1992).
27. D. R. Reichman, P. Charbonneau, *J. Stat. Mech.* **2005**, P05013 (2005).
28. T. R. Kirkpatrick, D. Thirumalai, P. Wolynes, *Phys. Rev. A* **40**, 1045 (1989).
29. J. P. Bouchaud, G. Biroli, *J. Chem. Phys.* **121**, 7347 (2004).
30. D. Kivelson, S. A. Kivelson, X. L. Zhao, Z. Nussinov, G. Tarjus, *Physica A* **219**, 27 (1995).

31. During the course of this work we have benefited from discussions with T. F. Miller III and F. van Wijland. The work was made possible through grants from the NSF (CHE-0543158 in the early stages for R.J. and D.C. and CHE-0626305 in the later stages for L.H. and D.C.), from the U.S. Office of Naval Research (N00014-07-1-0689 in the late stages for R.J.), and from the Engineering and Physical Sciences Research Council (GR/S54074/01 for J.P.G.).

Supporting Online Material

www.sciencemag.org/cgi/content/full/1166665/DC1
SOM Text
Figs. S1 to S4
References

1 October 2008; accepted 22 January 2009
Published online 5 February 2009;
10.1126/science.1166665
Include this information when citing this paper.

Functional Proteomics Identify Cornichon Proteins as Auxiliary Subunits of AMPA Receptors

Jochen Schwenk,[1]* Nadine Harmel,[1]* Gerd Zolles,[1]* Wolfgang Bildl,[1] Akos Kulik,[4] Bernd Heimrich,[4] Osamu Chisaka,[6] Peter Jonas,[3] Uwe Schulte,[1,2] Bernd Fakler,[1,5]† Nikolaj Klöcker[1]†

Glutamate receptors of the AMPA-subtype (AMPARs), together with the transmembrane AMPAR regulatory proteins (TARPs), mediate fast excitatory synaptic transmission in the mammalian brain. Here, we show by proteomic analysis that the majority of AMPARs in the rat brain are coassembled with two members of the cornichon family of transmembrane proteins, rather than with the TARPs. Coassembly with cornichon homologs 2 and 3 affects AMPARs in two ways: Cornichons increase surface expression of AMPARs, and they alter channel gating by markedly slowing deactivation and desensitization kinetics. These results demonstrate that cornichons are intrinsic auxiliary subunits of native AMPARs and provide previously unknown molecular determinants for glutamatergic neurotransmission in the central nervous system.

Fast excitatory synaptic transmission in the mammalian CNS is mostly mediated by AMPA receptors (AMPARs), ligand-gated ion channels that are activated by glutamate released from the presynaptic terminals (*1*–*4*). On activation, AMPARs provide the transient excitatory postsynaptic current (EPSC) that depolarizes the membrane and initiates downstream processes, such as the generation of action potentials or synaptic plasticity (*5*, *6*). The time course and amplitude of AMPAR-mediated EPSCs exhibit considerable variability among neurons and synapses and strongly depend on the properties of the postsynaptic AMPARs (*7*, *8*).

AMPARs are tetrameric assemblies of α subunits with distinct properties that are encoded by the glutamate receptor (GluR) genes GluR-A to GluR-D (*9*–*11*) [or GluA1-4 according to the International Union of Basic and Clinical Pharmacology nomenclature (*12*)] and their variations resulting from alternative splicing and RNA editing (*13*–*15*). In most central neurons, multiple variants of these GluR proteins are expressed and assembled into heteromultimeric channels that display a wide range of gating kinetics and Ca^{2+} permeabilities (*16*–*19*). In addition to the α subunits, the properties of the AMPARs are modulated by a family of transmembrane AMPAR regulatory proteins (TARPs) (*20*, *21*). The TARPs coassemble with the GluR proteins and through direct protein-protein interactions affect the gating, permeability and pharmacology of the AMPARs (*21*–*25*). Furthermore, the TARPs influence the number and subcellular localization of AMPARs by promoting their trafficking to the plasma membrane and their targeting to the synapse (*26*, *27*).

The profound impact of the TARPs led to the assumption that almost all AMPARs in the mammalian brain may be assembled with these auxiliary subunits (*28*, *29*). However, only a minor portion of the AMPAR complexes in the rat brain (~30%) are associated with γ-2 and γ-3, the TARPs with the most widespread expression pattern (*30*, *31*) (Fig. 1A, arrowhead). It is, therefore, possible that native AMPARs contain further yet-unknown protein constituents that may be iden-

[1]Institute of Physiology II, University of Freiburg, Engesserstrasse 4, 79108 Freiburg, Germany. [2]Logopharm GmbH, Engesserstrasse 4, 79108 Freiburg, Germany. [3]Institute of Physiology I, University of Freiburg, Engesserstrasse 4, 79108 Freiburg, Germany. [4]Institute of Anatomy and Cell Biology, University of Freiburg, Albertstrasse 23, 79104 Freiburg, Germany. [5]Center for Biological Signaling Studies (bioss), Albertstrasse 10, 79104 Freiburg, Germany. [6]Department of Cell and Developmental Biology, Kyoto University, Kyoto 606-8502, Japan.

*These authors contributed equally to this work.
†To whom correspondence should be addressed. E-mail: bernd.fakler@physiologie.uni-freiburg.de (B.F.) or nikolaj.kloecker@physiologie.uni-freiburg.de (N.K.)